ACS APPLIED MATERIALS & INTERFACES

Research Article

www.acsami.org

Introduction of Bifunctional Groups into Mesoporous Silica for Enhancing Uptake of Thorium(IV) from Aqueous Solution

Li-Yong Yuan, Zhi-Qiang Bai, Ran Zhao, Ya-Lan Liu, Zi-Jie Li, Sheng-Qi Chu,[†] Li-Rong Zheng,[†] Jing Zhang,[†] Yu-Liang Zhao, Zhi-Fang Chai,*[,‡] and Wei-Qun Shi*

Key Laboratory of Nuclear Radiation and Nuclear Energy Technology and Key Laboratory for Biomedical Effects of Nanomaterials & Nanosafety, Institute of High Energy Physics, Chinese Academy of Sciences, Beijing 100049, China

Supporting Information

ABSTRACT: The potential industrial application of thorium (Th), as well as the environmental and human healthy problems caused by thorium, promotes the development of reliable methods for the separation and removal of Th(IV) from environmental and geological samples. Herein, the phosphonate-amino bifunctionalized mesoporous silica (PAMS) was fabricated by a one-step self-assembly approach for enhancing Th(IV) uptake from aqueous solution. The synthesized sorbent was found to possess ordered mesoporous structures with uniform pore diameter and large surface area, characterized by SEM, XRD, and N_2 sorption/desorption measurements. The enhancement of Th(IV) uptake by PAMS was achieved by coupling of an access mechanism to a complexation mechanism, and the sorption can be optimized by adjusting the coverage of the functional groups in the PAMS sorbent. The systemic study on Th(IV) sorption/desorption by using one coverage of PAMS (PAMS12) shows that the Th(IV) sorption by PAMS is fast with equilibrium time of less than 1 h, and the sorption capacity is more than 160 mg/g at a relatively low pH. The sorption isotherm has been successfully modeled by the Langmuir isotherm and D-R isotherm, which reveals a monolayer homogeneous chemisorption of Th(IV) in PAMS. The Th(IV) sorption by PAMS is pH dependent but ionic strength independent. In addition, the sorbed Th(IV) can be completely desorbed using 0.2 mol/L or more concentrated nitric acid solution. The sorption test performed in the solution containing a range of competing metal ions suggests that the PAMS sorbent has a desirable selectivity for Th(IV) ions.

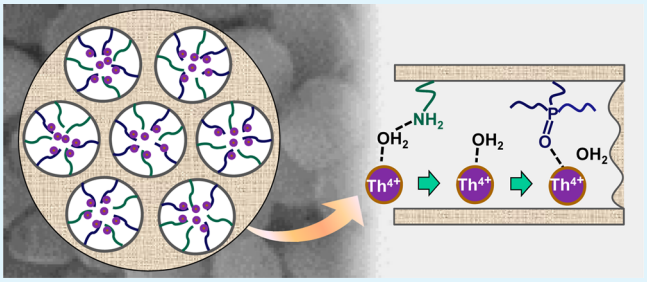

KEYWORDS: *mesoporous silica, bifunctionality, phosphonate, amino, thorium, sorption*

INTRODUCTION

Mesoporous materials, i.e., porous materials with pore size at 2.0−50 nm, such as MCM-41, have attracted much attention in various scientific areas in the past two decades.[1−6] Especially, ordered mesoporous silica materials are novel families of the fascinating porous solids, which have very high specific surface areas, thermal and mechanical stability, highly uniform pore distribution and tunable pore size, high sorption capacity, and unprecedented hosting properties, as well as extraordinarily wide possibilities of functionalization.[7−9] These advantages make the ordered mesoporous silica an ideal supporting material for the metal ion extraction. With the recent renaissance of nuclear energy, the mesoporous silica materials were also widely applied to the preconcentration and/or separation of actinides.[10,11]

Among actinides, thorium is an important natural radioactive element with larger abundance than uranium. ^{232}Th will be a better fertile material than ^{238}U and can breed fissile material more efficiently, for which thorium is receiving an ever-increasing interest recently as a fertile material for producing nuclear fuel. Besides, the toxic nature of thorium, even at trace levels, has been a public health problem by causing acute toxicological effects and harmful diseases. Thorium is also an important model element for tetravalent actinides such as Np(IV), U(IV), and Pu(IV), which do not always keep in tetravalent form and thus are difficult to handle. All these issues require the investigations of preconcentration, separation, and recovery of thorium from environmental and geological samples.

The recovery and preconcentration of thorium have been reported using solid phase extraction (SPE).[12−14] Especially in the past decade, a number of sorbents including mesoporous silica have been developed for Th(IV) sorption. Zuo[15] et al., for example, studied the sorption of Th(IV) on mesoporous molecular sieves (Al-MCM-41). The results showed that the sorption of Th(IV) on Al-MCM-41 is a spontaneous and endothermic process, and the sorption achieves equilibrium in 12 h. Yousefi[8] et al. reported 5-nitro-2-furaldehyde modified MCM-41 as sorbent for solid phase extraction of Th(IV) from aqueous solution. The maximum sorption capacity reached 49

Received: December 5, 2013
Accepted: March 12, 2014
Published: March 12, 2014

   dx.doi.org/10.1021/am405584h | ACS Appl. Mater. Interfaces 2014, 6, 4786−4796

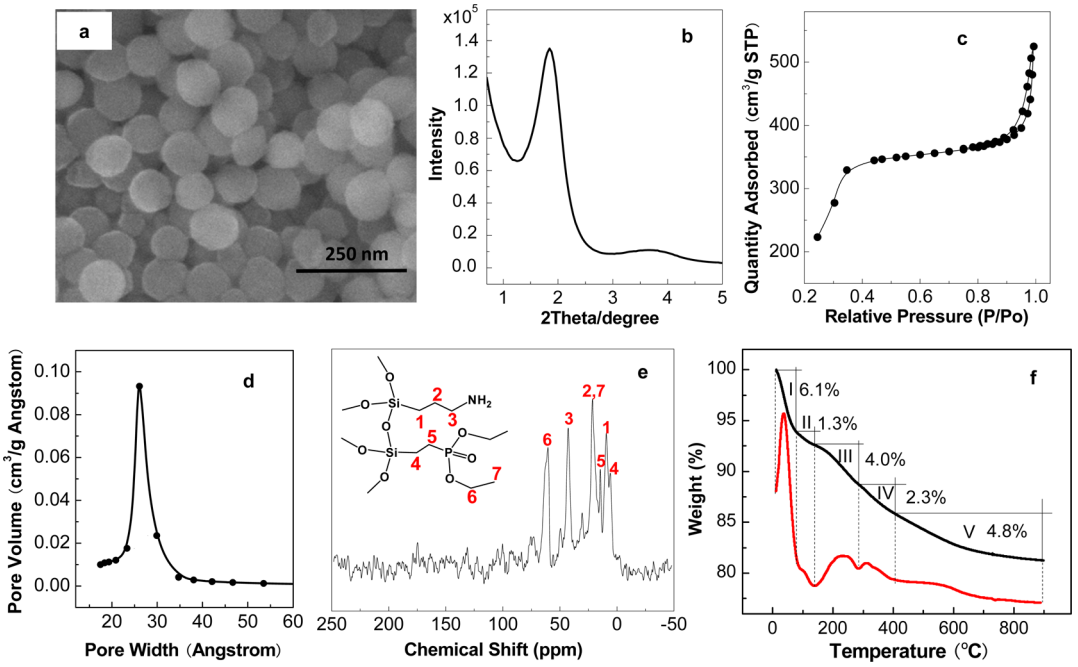

Figure 1. Characterizations of PAMS12. (a) SEM image, (b) XRD pattern, (c) N_2 sorption/desorption isotherm, (d) pore size distribution, (e) ^{13}C CP/MAS NMR spectra, and (f) TGA profile.

mg/g at pH 5.5. These works have dealt with the sorption of Th(IV) by using mesoporous silica. The sorption capacities and/or sorption kinetics, however, are not satisfactory, which depends on the functionalization of the mesoporous silica.

The organically functionalized mesoporous silica materials are generally fabricated by postsynthetic functionalization of silica (grafting) and one-pot template directing synthesis (co-condensation). The co-condensation method has a number of advantages such as without exciting pore blocking and homogeneous organic unit distribution. Recently, we reported the synthesis of phosphonate functionalized mesoporous silica through co-condensation method for solid extraction of actinides ions,[16] from which we found that the availability of phosphonate modified onto mesoporous silica is somewhat low. That is, not all phosphonate groups on the surface of sorbent interact with target metal ions. This probably results from the presence of inner cavity in mesoporous silica. Free phosphonate groups exist in the inner cavity that the target metal ions cannot reach easily due to the narrow diameter of the pores (2−3 nm for typical MCM-41). In this work, we simultaneously introduced amino group and phosphonate group into mesoporous silica (PAMS) by one-step co-condensation method for attempting to improve the availability of functional group on the sorbent and thus enhance Th(IV) uptake from aqueous solution. The Th (VI) sorption by different functionalized mesoporous silica and PAMS at various coverage of the functional group was compared and the sorption mode of Th(IV) in PAMS was discussed in detail. Further, the effect of various parameters such as contact time, pH, ion strength, and initial Th(IV) concentration on the sorption, as well as the desorption of Th(IV) from PAMS and the selectivity of PAMS for Th(IV), were investigated in detail. The present results indicate a better scope by introducing multifunctionality into mesoporous silica for the separation of actinide ions from environment.

EXPERIMENTAL SECTION

Chemical Materials. Tetraethoxysilane (TEOS), cetyltrimethylammonium bromide (CTAB), N-acyl-glutamic sodium (C_{18}GluS), and polyethylene glycol monocetyl ether (Brij56) were obtained from Sinopharm Chemical Reagent Co.,Ltd. (SCRC), China. Diethylphosphato-ethyltriethoxysilane (DPTS) and 3-aminopropyltrimethoxysilane (APS) were purchased from Tokyo Chemical Industry Co., Ltd. (TCI), Japan. Thorium nitrate ($Th(NO_3)_4{\cdot}4H_2O$) was purchased from China Minmetals (Beijing) Research. All these materials were used as received. The Th(IV) stock solution was prepared by dissolving the appropriate amounts of $Th(NO_3)_4{\cdot}4H_2O$ in 0.5 M HNO_3. All other chemicals were of analytical grade and used without further purification. Deionized water used in all experiments was obtained from the Milli-Q water purification system.

Synthesis of Mesoporous Silica. Phosphonate-amino bifunctionalized mesoporous silica (PAMS) was synthesized by co-condensation of DPTS, APS and TEOS using CTAB as the template. In a typical synthesis, 0.364 g of CTAB was dissolved in 100 mL of 14 mmol/L sodium hydroxide. The suspension was evenly mixed, and 2.08 g of TEOS, 0.197 g of DPTS, and 0.107 g of APS were added subsequently. The reactant composition in mole was 1:10:0.6:0.6 CTAB:-TEOS:DPTS:APS. After 4 h of vigorous stirring at 353 K, the mixture was transferred to a Teflon bottle and heated at 373 K for 2 days. Then the solid phase was recovered by filtration, washed with distilled water, dried at 333 K, and extracted by a mixed solution of hydrochloric acid and alcohol. Thus derived sample was named PAMS12, corresponding to the nominal (DPTS + APS)/TEOS molar ratio of 12%.

Phosphonate functionalized mesoporous silica (NP10) was synthesized by co-condensation of DPTS and TEOS using CTAB as the template. Amino-functionalized mesoporous silica was prepared by grafting APS into a typical synthesized SBA-15 (APSS), and by co-condensation of APS and TEOS using a mixture of C_{18}GluS and Brij56 as the template (AMS-11), respectively. The details on the preparation of NP10 and APSS were reported in our pervious works.[16,17] In a typical synthesis of AMS-11, 0.3 g of Brij56 and 0.94 mL of 1 mol/L hydrochloric acid were added into 42 g of water. After complete dispersion at 353 K, 0.414 g of C_{18}GluS and then 0.358 g of APS, 3.12 g of TEOS were added with vigorous stirring for 30 min. The mixture was aged for 1 day at 353 K in a Teflon bottle. Then the solid phase

dx.doi.org/10.1021/am405584h | ACS Appl. Mater. Interfaces 2014, 6, 4786−4796

was recovered by filtration, washed with distilled water, dried at 333 K, and extracted by a mixed solution of alcohol and ethanolamine. MCM-41 was prepared according to a typical procedure as reported previously.[18,19]

Analytical Techniques. The synthesized mesoporous silica was characterized by scanning electron microscopy (SEM), powder X-ray diffraction (XRD), N_2 sorption/desorption isotherm experiments, nuclear magnetic resonance (NMR), thermogravimetric analysis (TGA) and Fourier transform infrared spectroscopy (FTIR). The Th (IV)-loaded mesoporous silica was tested by Extended X-ray absorption fine structure (EXAFS) and FTIR. The residual concentration of tested ion(s) in supernatants in the selectivity test experiment were determined by inductively coupled plasma mass spectrograph (ICP-MS), while the quantitative determination of Th(IV) in single component sorption experiments was performed by spectrophotometric method using arsenazo-III as the complexing agent at a wavelength of 672 nm. Detailed illustrations on the analytical techniques were listed in SI-1 in the Supporting Information.

Sorption Experiments. The sorption experiments were carried out using the batch method at room temperature. The Th(IV)-solutions were prepared by diluting the Th(IV) stock solution to suitable concentrations depending on the experimental requirements. The values of pH were adjusted by adding negligible volumes of diluted nitric acid or sodium hydroxide. The control experiment was performed at the same time by using the identical Th(IV) solution in the absence of the sorbent. Detailed experimental procedure is described in Supporting Information SI-2 and some experimental conditions are presented in the related figure and table captions for clear identification.

RESULTS AND DISCUSSION

Morphological and Structural Characterizations. The characterizations of the PAMS12 sample are shown in Figure 1. The SEM image indicates that the sample is composed of spherical nanoparticle with an average particle size of ca. 80 nm. The XRD pattern shows one sharp peak in the range of 2θ close to 2.0 and one broad peak in the region of 2θ = 3−5°, which reveals the presence of ordered mesoporous structure. The surface area, primary mesopore volume and pore size are 741m^2/g, 0.976 cm^3/g, and 2.6 nm, respectively, determined by nitrogen sorption. The nitrogen sorption/desorption isotherm is type IV, typical for a mesoporous material. All the resonance signals in the ^{13}C CP/MAS NMR spectra can be assigned to appropriate C atoms of DPTS and APS, as denoted in Figure 1e, which shows that a phosphonate-amino bifunctionalized mesoporous material has been successfully prepared.

Another evidence for the expected material is from FTIR, as shown in Figure 4. Although the absorption bands assigned to phosphonate, i.e., P═O and P−O−R stretching mode, are immerged into the siloxane peak, leading to an intensity increase at the range of 1300−1000 cm^{-1} after normalization with native material, the absorption bands assigned to C−H and N−H stretching mode appear at 2930 and 1520 cm^{-1}, respectively. Besides, a small band that represents the bending vibration of C−H bond is revealed at 1412 cm^{-1}, and an increase of the absorption at 3200−3600 cm^{-1} induced by the hydrogen-bonded R-NH_2 is clearly denoted. All the observations further confirm that the expected functional groups are anchored to the surface of silica.

To determine the amount of functional groups in the prepared material, thermal analyses for PAMS12 sample was performed in the temperature range of 20−900 °C. The result is shown in Figure 1f. It is found that the weight loss of PAMS12 with the increase in temperature shows five distinct stages, as clearly denoted by the derivation of weight loss (red line in Figure 1f). The first two stages at temperatures below 200 °C can be attributed to the volatilization of physically adsorbed water and organic solvent outside (stage I) and inside (stage II) the pores, respectively. At temperatures above 200 °C, the weight loss sharply increases, and two most significant weight loss points appear in tandem in the temperature of ca. 250 and 320 °C, corresponding to stage III and stage IV. The two stages are reasonably assigned to the pyrolysis of the attached phosphonate and amino groups, respectively, on the pore outside surface of PAMS12 since the most significant weight loss of phosphonate-functionalized mesoporous silica (NP10) and amino-functionalized mesoporous silica (APSS) occur in the same temperature range (see Supporting Information SI-3, Figure 1S). Such a result provides another evidence that two kinds of functional groups are attached on the prepared material. Further, a weight loss of 4.0% is observed at the temperature above 400 °C, which reasonably arises from the pyrolysis of the attached functional groups inside the pores (stage V). At or near 800 °C, the TGA profile reaches a plateau, and the total weight loss is about 11.1% except the volatilization of water and organic solvent. Although the pyrolysis of phosphonate and amino groups in stage V are not differentiated each other, the coverage of the functional groups can still be calculated according to stage III and stage IV since the prepared material is considered to be homogeneous. In detail, the weight loss of 4.0% in stage III versus 2.3% in stage IV suggests that the pyrolysis of phosphonate group contributes to ca. 63.5% of total weight loss and the rest is assigned to the pyrolysis of amino group, from which the coverage of phosphonate group and amino group can be calculated to be 0.43 and 0.70 mmol/g, respectively (the molecular mass of triethylphosphate and propylamine functional groups are 165 u and 58 u, respectively).

Th(IV) Sorption. *Comparison of Unfunctionalized and Various Functionalized Mesoporous Silica.* The sorption of Th(IV) by APSS, AMS-11, NP10 and PAMS12, as well as unfunctionalized MCM-41 at the same pH (3.5 ± 0.1) and initial Th(IV) concentration (120 mg/L) were compared in Figure 2. It is observed that the performance of unfunctionalized MCM-41 for Th(IV) sorption is not the worst in the test sorbents, which can be rationalized from the large surface areas of MCM-41 (as denoted by nitrogen sorption/desorption experiment in Supporting Information SI-4, Figure 2S) and the exposed silanol group on the surface of MCM-41 (as indicated by FTIR analysis in Figure 4). It is well-known that Th(IV) ions, like other actinide ions, readily form complexes with O-

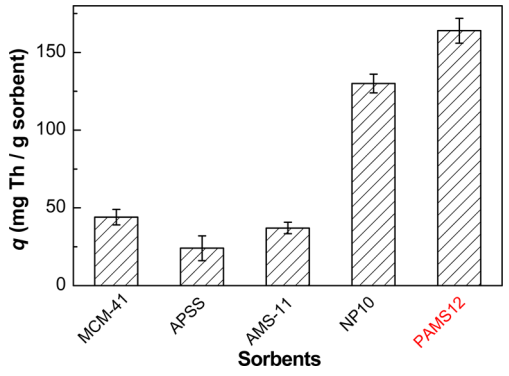

Figure 2. Comparison of Th(IV) sorption by unfunctionalized and various functionalized mesoporous silica under the same conditions ($m_{sorbent}/V_{solution}$ = 0.4 mg/mL, $[Th]_{initial}$ = 120 mg/L, pH 3.5 ± 0.1).

donor ligand. The silanol group on the surface of MCM-41 may serve as an O-donor ligand for complexation with Th(IV) ions, thus leading to a reasonable Th(IV)sorption. The contribution of exposed silanol group in the mesoporous silica to the actinides sorption is well reported by us[16,20] and other researchers.[10] After amino-modification, regardless of by co-condensation (AMS-11) or by grafting (APSS), the Th(IV) uptake did not increase but even decreased compared with that of MCM-41. This is an unexpected result. We consider that the Th(IV) sorption by AMS-11 and APSS is also mainly contributed to the exposed silanol group. The consideration is based on the following two facts. One fact is that both AMS-11 and APSS contain some free silanol groups, which can be revealed by the broad absorption band at 3200−3600 cm^{-1} and a small band at ~960 cm^{-1} in FTIR as shown in Figure 3. The

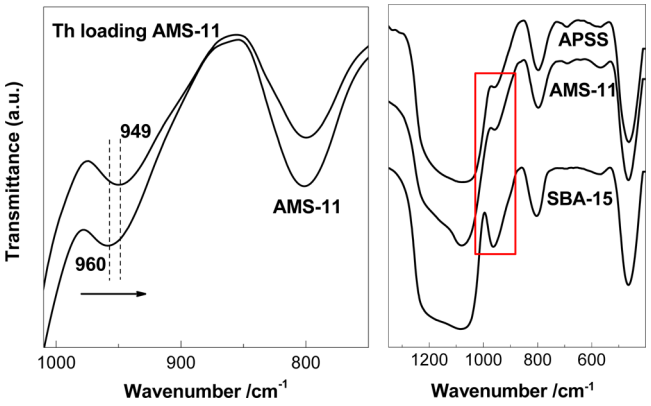

Figure 3. Left: FTIR of as-synthesized AMS-11 and Th (IV)-loaded AMS-11. Right: FTIR of as-synthesized AMS-11, APSS, and MCM-41.

contribution of exposed silanol group in the mesoporous silica to the actinides sorption is well-known as mentioned above and was also indicated by the present results. Figure 3 (left) shows the FTIR of as-synthesized AMS-11 and Th(IV)-loaded AMS-11, from which we can see that the absorption band assigned to O−H of silanol group at ~960 cm^{-1} shifted to ~949 cm^{-1} after Th(IV) sorption. This is an indication of the interaction between silanol group and Th (IV). Another fact is that increasing the coverage of amino group on the surface of the sorbent by increasing APS amount in the reaction mixture does not benefit the Th(IV) sorption (see latter section), which suggests that amino group is not the main complexation ligand. Taken together, it is deemed that amino group is not an effective Th(IV) ligand, and the exposed silanol group on the surface of APSS and AMS-11 mainly contributes to the Th(IV) sorption. Compared to unfunctionalized MCM-41, however, less amount of silanol group remain on the APSS and AMS-11 sorbent due to the introduction of large amount of amino group (2.07 and 2.76 mmol/g, respectively), evidenced by the obvious intensity drop of the absorption band assigned to silanol at ~960 cm^{-1} as shown in Figure 3 (right). Thus, a poor Th(IV) uptake of less than 40 mg/g is expected.

When the mesoporous silica was modified by phosphonate (NP10), the Th(IV) uptake reaches 130 mg/g, a value even two times larger than that of MCM-41. The result firmly shows that the performance for the Th(IV) sorption is significantly improved by introducing an effective Th(IV) ligand of phosphonate. What is more, the improvement of Th(IV) sorption is further enhanced after comodification by phosphonate and amino group (PAMS12), and the largest Th(IV) uptake of 164 mg/g was obtained. This is an interesting result. As mentioned above, amino group almost does not complex with Th(IV) ions. And the amount of phosphonate group in PAMS12 (0.43 mmol/g, denoted by TGA in Figure 1e) is obviously lower than that of NP10 (0.55 mmol/g, calculated from the TGA measurement in Supporting Information SI-3), but the Th(IV) uptake by PAMS12 is more effective than that by NP10.

To rationalize the results, we recorded the FTIR spectra of Th(IV)-loaded PAMS12 and NP10, as shown in Figure 4. Also

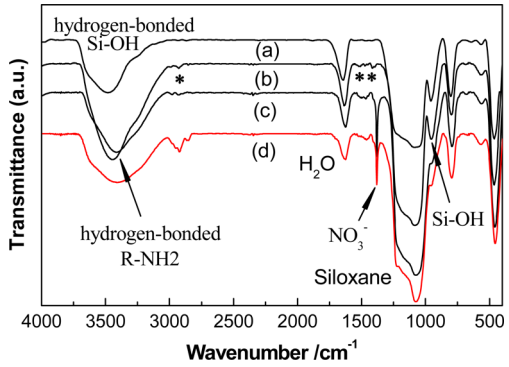

Figure 4. FTIR of (a) as-synthesized MCM-41, (b) PAMS12, (c) Th(IV)-loaded PAMS12, and (d) Th(IV)-loaded NP10.

shown in Figure 4 are the FTIR spectra of as-synthesized MCM-41 and PAMS12. It is well-known that the oxygen of phosphonate readily binds actinides, generally leading to the IR absorption changes. But unfortunately in this work, both P═O and P−O−R stretching mode of phosphonate are immerged into the siloxane peak, which does not allow for the observation how they change during Th(IV) sorption. However, the similarity of the spectra of Th (IV)-loaded PAMS12 and NP10 in all ranges seems to give a hint that PAMS and NP10 sorb Th(IV) in a similar way. Besides, when compared to the FTIR of Th (IV)-loaded PAMS12 with that of as-synthesized PAMS12, there are two obvious differences. One is that a sharp peak at ~1380 cm^{-1} appears. The other is that the absorption band assigned to O−H of silanol group at ~960 cm^{-1} shifts toward low wavenumber and shows an obvious intensity drop. The former difference clearly suggests that nitrate anions as counterions of Th(IV) were cosorbed by the sorbent, while the latter difference gives an indication that silanol group in the sorbent binds Th(IV) by forming O-M bond, leading to an absorption shifting and intensity drop. Such a result is well-consistent with our expectation that the reasonable Th(IV) sorption by MCM-41, AMS-11, and APSS is attributed to the exposed silanol group on the surface of sorbent.

Besides, EXAFS spectra of Th(IV)-loaded PAMS12 and NP10 were compared to further identify the sorption mode of Th(IV) onto PAMS12 (Figure 5). As reference, the spectra of as-prepared Th(IV) hydroxide precipitate were also provided in Figure 5 (Details on the preparation and EXAFS measurement are present in Supporting Information SI-1). It is observed that spectra A and B show almost the same oscillation mode and the same intense FT peaks at the range of 1−4 Å (not phase correction), but are obviously different from the reference one of Th(IV) hydroxide precipitate. This indicates that PAMS12 and NP10 sorbed Th(IV) in a same way and Th(IV) did not noticeably precipitate from the suspension under the

dx.doi.org/10.1021/am405584h | ACS Appl. Mater. Interfaces 2014, 6, 4786−4796

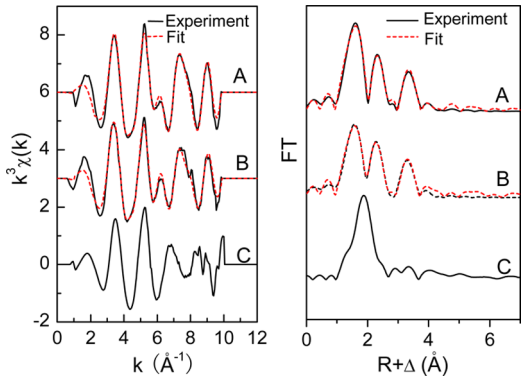

Figure 5. Left: Raw Th L_{III}-edge k^3 weighted EXAFS spectra of Th sorbed to (A) PAMS12 and (B) NP10 including the best theoretical fits and (C) as-prepared Th(IV) hydroxide precipitate as reference. Right: Corresponding Fourier transforms. The FT spectra are not corrected for phase shift.

experimental conditions. Reasonable fittings of spectra A and B are then followed and the metric parameters are presented in Table 1. As can be seen, Th(IV) sorbed to PAMS12 and NP10 have almost the same metric parameters. Specially, 5−6 oxygen atoms at ∼2.47 Å comprise the first coordination shell of the Th(IV) ions sorbed on the PAMS and NP10 sorbents, and the Th−O distance obtained in this work is in agreement with that reported in previous literatures.[21,22] ∼1 phosphorus atom at ∼3.1 Å represents the second coordination shell of the Th(IV) ions, and the Th−P distance is well-consistent with that in reported $Th[PO_4][OH]$ crystal.[23] Finally, the multiple scattering of Th−O−P contributes the rest FT peaks at distance more than 3.1 Å. All the fitting results direct the coordination of Th(IV) with phosphonate group for both PAMS12 and NP10.

Table 1. Metric Parameters Extracted by Least-Squares Fitting Analysis of EXAFS

sample	shell	CN[a]	R (Å)[b]	σ^2/ Å^2[c]	ΔE(eV)[d]	R-factor[e]
A	Th−O	5.1	2.47	0.0150	3.6	0.0061
	Th−P	0.7	3.12	0.0022	15.9	
	Th−O−P	4.4	3.98	0.0110	15.9	
B	Th−O	5.9	2.48	0.0134	4.0	0.0058
	Th−P	0.8	3.10	0.004	13.8	
	Th−O−P	4.0	3.96	0.010	13.8	

[a]Coordination number. $N \pm$ ∼20%. [b]Interatomic distance. $R \pm$ ∼0.03 Å. [c]Debye−Waller factor. [d]Energy shift linked for all the paths except the first shell paths. [e]Goodness of fit parameter.

From the above characterizations and the fact that increasing the coverage of the amino group on the surface of the sorbent by increasing the APS amount in the reaction mixture does not benefit the Th(IV) sorption (see latter section), it is obvious that the Th(IV) uptake by both PAMS12 and NP10 mainly occurs in the same way through the complexation of Th(IV) with oxygen of the phosphonate group. Nevertheless, the difference between the sorption capacity of NP10 and PAMS12 also clearly suggests that the amino group in PAMS12 plays important roles during Th(IV) sorption. For NP10, i.e. solely phosphonate functionalized mesoporous silica, 0.55 mmol/g of phosphonate produces a saturated capacity of 130 mg/g for Th(IV). Since the exposed silanol group also contributes partly to the Th(IV) uptake as evidenced by FTIR (Figure 4), it is clear that not all phosphonate groups were bound to Th (IV) even if in 1:1 complexation mode. Free phosphonate groups may exist in the inner cavity of the NP10 sorbent, and Th(IV) ions cannot reach these sites easily due to the narrow diameter of the pores (ca.2.6 nm). For PAMS12, however, the amount of phosphonate group is calculated to be 0.43 mmol/g by thermal analyses, while the saturated capacity for Th(IV) reaches more than 160 mg/g. According to total BET surface area of PAMS12 (741 m^2/g), an average coverage of 0.35 phosphonate molecule/nm^2 along with a distance between two phosphonate molecules of more than 1.7 nm is calculated. The distance is so large that one Th(IV) ion cannot interact with two or more phosphonate molecules, revealing that phosphonate: Th(IV) = 1:1 is an exclusive complexation mode on the PAMS12 sorbent. Accordingly, 0.43 mmol/g of phosphonate only contributes to ca.100 mg/g of Th(IV) uptake even if all phosphonate groups bind Th(IV). The rest, ca.60 mg/g, can but be reasonably attributed to the exposed silanol group on the sorbent surface. Such a result means that amino group in PAMS12 enhances Th(IV) uptake by improving the availability of complexation ligand on the sorbent. Introduction of bifunctionality into some ion-exchange resins for enhancing metal ion complexation have been reported by several investigators,[24−26] in which the enhanced effect is attribute to coupling of an access mechanism to a complexation mechanism. Similarly in this work, the introduction of more hydrophilic amino group increases the hydrophilicity of the sorbent and thus provides a more convenient access mechanism for Th(IV) ions into the inner cavity of the sorbent. In this case, more phosphonate groups interact with Th(IV) ions and sequestrate them, thus inciting an enhanced Th(IV) sorption. Besides, this access mechanism also works for the exposed silanol group. In unfunctionalized MCM-41, the exposed silanol group provides a saturated capacity of 44 mg/g for Th (IV), while in PAMS12, the exposed silanol contributes to ca.60 mg/g Th(IV) uptake. That is, the incorporated amino group acts as an access ligand to gain entry of Th(IV) ions into the inner cavity of the sorbent, and more silanol groups in the pores bind Th(IV), thus increasing Th(IV) uptake.

Comparison of Phosphonate-Amino Bifunctionalized Mesoporous Silica at Different Coverage. The above results clearly show that the combination of phosphonate and amino groups in PAMS12 arouses an enhancement of Th(IV) uptake. In this case, increasing the total amount of the two functional groups on the sorbent may further enhance Th(IV) uptake.

Table 2. Summary of Th(IV) uptake by PAMS Series, Phosphonate and Amido Coverage, As Well As Structural Parameters Obtained by the Measurement of N_2 Sorption/Desorption

sample	Th(IV) uptake (mg/g)	phosphonate (mmol/g)	amido (mmol/g)	BET surface area (m^2/g)	pore volume (cm^3 /g)	Pore size (nm)
PAMS-12	164	0.43	0.70	741	0.976	2.6
PAMS-18	110	0.31	1.25	670	0.903	2.5
PAMS-24	97	0.32	1.47	605	0.702	2.3

Herein, PAMS18 and PAMS24 were prepared following the same procedure as that used for PAMS12, except that different amount of functional reagents (DPTS:APS = 1:1 in mole) were added to reach the nominal (DPTS + APS)/TEOS molar ratio of 18 and 24%, respectively. The results of Th(IV) uptake using the prepared PAMS series were compared in Table 2. As can be seen that the Th(IV) uptake was not increased as expected but decreased with increasing the amount of DPTS and APS in reaction mixture. For PAMS 24, the Th(IV) uptake was even decreased to less than 100 mg/g, a value only half of that for PAMS12.

To probe how the decrease occurred, we performed the thermal analyses of PAMS18 and PAMS24 (Figure 6), and the

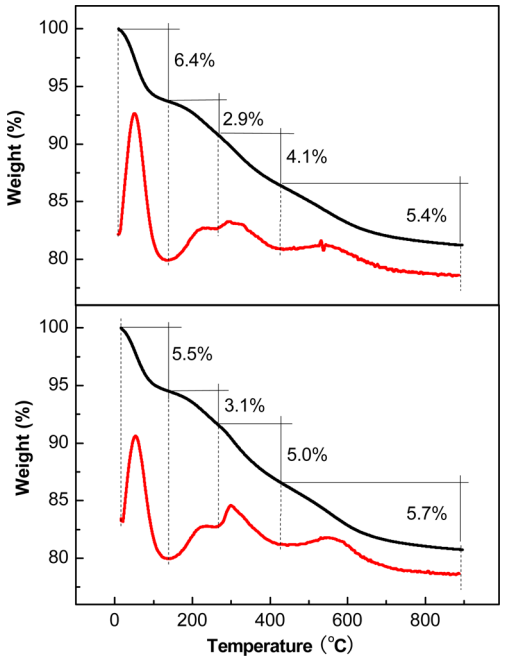

Figure 6. TGA profiles of PAMS18 (top) and PAMS24 (bottom).

N_2 sorption/desorption isotherm, as well as recorded XRD pattern of PAMS18 and PAMS24 (Figure 7). From thermal analyses, it is observed that the weight loss of PAMS18 and PAMS24 at the temperature range of 200−800 °C increase to 12.4 and 13.8%, respectively, revealing a higher total coverage of functional groups than PAMS12. Following the same method as that used for PAMS12, the coverage of phosphonate group and amino group in PAMS18 and PAMS24 was calculated, respectively, as listed in Table 2. It can be seen that the coverage of amino group rises obviously from 0.7 mmol/g for PAMS12 to 1.47 mmol/g for PAMS24, the increment is more than one time. The coverage of phosphonate group, however, does not rise but drops from 0.43 mmol/g for PAMS12 to less than 0.35 mmol/g for PAMS18 and PAMS24. Such a result seems to give a hint that amino group is more liable than phosphonate group to be modified onto mesoporous silica, probably because of its small size. When increases the amount of DPTS and APS by the same ratio in the reaction mixture, the competition between phosphonate group and amino group finally decreases the coverage of phosphonate group on the surface of the PAMS sorbent. Whatever, the different coverage of functional groups on the surface of the sorbents should be responsible for the drop of the Th(IV) sorption by PAMS18 and PAMS24. That is, the increase of the amino group coverage does not benefit the Th(IV) uptake, whereas the drop of the phosphonate groups brings negative effects on the Th(IV) uptake. The result gives another support for our conclusion that phosphonate group but not amino group should be responsible for the complexation with Th(IV) during sorption. On the other hand, the N_2 sorption/desorption isotherm(Figure 7 left and Table 2) clearly suggested that the surface area and primary mesopore volume, as well as the pore size of PAMS18 and PAMS24 are decreased compared with that of PAMS12, which is known to be bad for the metal ions sorption. The XRD patterns (Figure 7 right) exhibit that the ordered structures of PAMS18 and PAMS24 are somewhat distorted, as evidenced by the intensity reduction of the peak in the range of 2θ close to 2.0 and the almost disappearance of the broad peak in the region of $2\theta = 3-5°$. All above issues are also responsible for the decrease of Th(IV) sorption.

In addition, the PAMS sorbents in the nominal (DPTS + APS)/TEOS molar ratio of less than 12%, such as PAMS10, were also prepared and used to Th(IV) sorption to further assess the effect of coverage of functional group on the sorption. It is understandable that the Th(IV) uptake by PAMS10 is not more than that of PAMS12 since the coverage of both phosphonate and amino groups in PAMS10 is less than that in PAMS 12, although the large surface area and ordered structure were maintained.

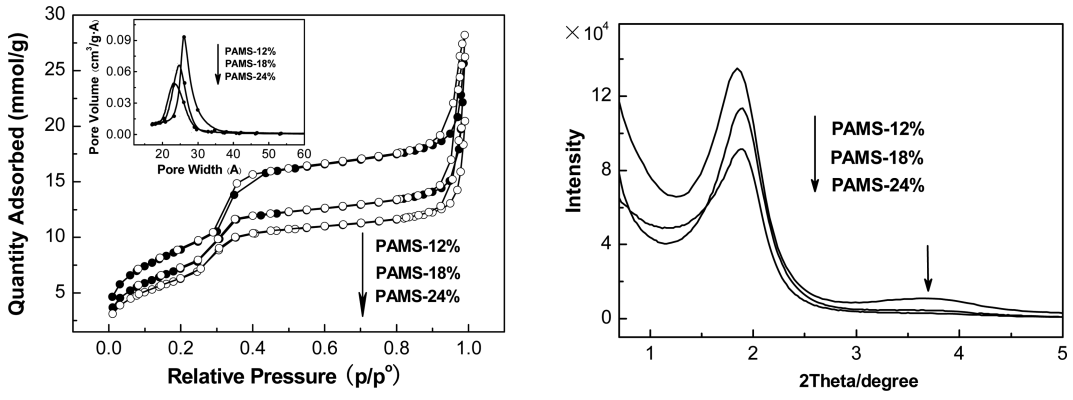

Figure 7. Comparison of N_2 sorption/desorption isotherm (left), pore size distribution (left inset), and XRD pattern (right) of PAMS12, PAMS18, and PAMS24.

dx.doi.org/10.1021/am405584h | ACS Appl. Mater. Interfaces 2014, 6, 4786−4796

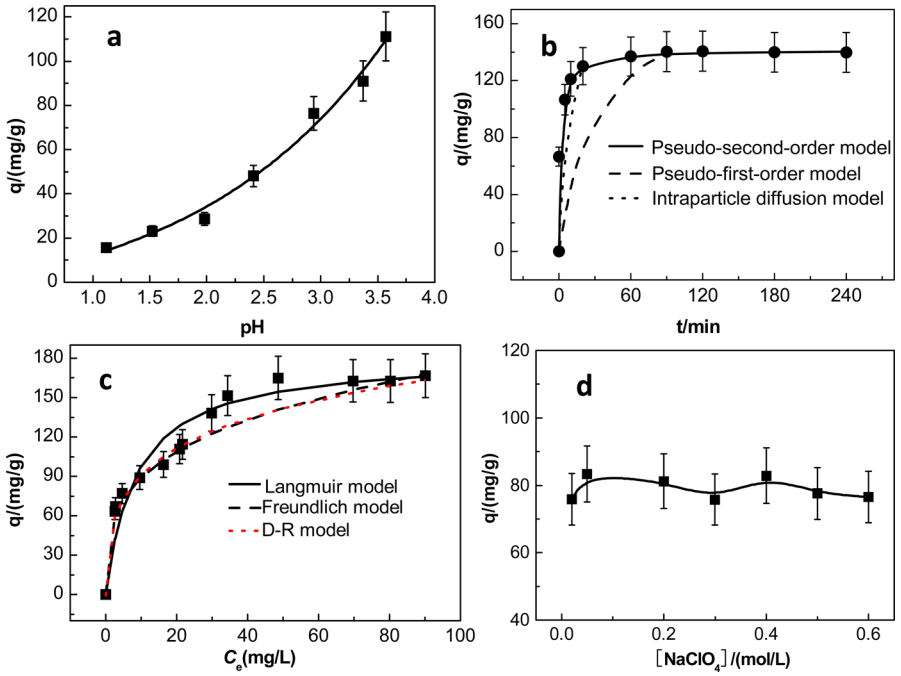

Figure 8. Th(IV) sorption by PAMS12 under various conditions. (a) Effect of pH, $m_{sorbent}/V_{solution}$ = 0.4 mg/mL; $[Th]_{initial}$ = 100 mg/L. (b) Sorption kinetics, $m_{sorbent}/V_{solution}$ = 0.4 mg/mL; pH 3.5 ± 0.1; $[Th]_{initial}$ = 100 mg/L. (c) Sorption isotherm, $m_{sorbent}/V_{solution}$ = 0.4 mg/mL; pH 3.5 ± 0.1. (d) Effect of ionic strength, $m_{sorbent}/V_{solution}$ = 0.1 mg/mL; pH 3.5 ± 0.1 $[Th]_{initial}$ = 20 mg/L.

Based on above analysis, more detailed adjustment on the raw material ratio in the reaction mixture may optimize the experimental conditions to obtain more effective Th(IV) sorbent. The related works are still going on in our laboratory. But from the present results, it is clear that the nominal (DPTS + APS)/TEOS molar ratio of 12% in reaction mixture is suitable for preparation of the phosphonate and amino bifunctionalized mesoporous silica as Th(IV) sorbent, from which the sorbent contains the suitable amount of functional groups and have large surface area and ordered structure, thus providing more effective Th(IV) sorption.

Systemic Study on Th(IV) Sorption/Desorption by Using PAMS12. *Th(IV) Sorption under Various Conditions.* To further evaluate the adsorptivity of PAMS sorbent, we conducted the sorption of Th(IV) from aqueous solution into PAMS12 under various conditions of pH, contact time, initial Th(IV) concentration, and ionic strength.

Figure 8a shows the results of Th(IV) sorption by PAMS12 at various pH. It can be seen that the uptake of Th(IV) markedly increases with increasing pH from 0.8 to 3.8. We rationalize the pH-dependent sorption with the surface charge of PAMS12 and the Th(IV) speciation. At lower pH, the phosphonate and amino groups on the surface of the sorbent are protonated and positively charged. The repulsive electrostatic interaction between the positively charged sorbent and the positively charged Th(IV) in aqueous solution leads to a low sorption. As pH increases, the phosphonate and amino groups are deprotonated, whereas Th(IV) still exists in positively charged form. The electrostatic interaction and complexation between the functional groups and Th(IV) incites the increase of the sorption. On the other hand, the species distribution of Th(IV) is greatly dependent on the pH of solution.[27,28] We calculated the aqueous and solid speciation of Th(IV) as a function of pH in the absence of sorbent according to the thermodynamic data reported previously,[29] as shown in Supporting Information SI-5. It is clear that at pH 3–4 and Th(IV) concentration of <0.5 mmol/L, the hydroxide complexes, $Th(OH)_2^{2+}$ and $Th(OH)^{3+}$, are the predominant species. These species may be more favored by the sorbent, thus leading to a higher sorption. Besides, the calculation shows that when the pH is over 3.7 and the total Th(IV) concentration exceeds 0.7 mmol/L, amorphous Th(IV) hydroxide or hydrous oxide precipitates from the solution. To avoid the precipitation of Th(IV) from the solution and also achieve higher Th(IV) sorption, the optimum pH 3.5 ± 0.1 and the initial Th(IV) concentration less than 0.7 mmol/L was used for the subsequent sorption experiments unless otherwise stated.

Effect of contact time, i.e., sorption kinetics, was studied at initial Th concentration ($[Th]_{initial}$) of 100 mg/L for contact time of 2 to 240 min. The results are shown in Figure 8b. As can be seen that the sorption of Th(IV) in PAMS12 is ultrafast especially in the initial several minutes, and the sorption process reaches equilibrium at around 1 h. The equilibrium time is close to that on MX-80 bentonite[30] and oxidized multiwalled carbon nanotubes,[31] but much faster than 12 h in Al-MCM-41,[15] 12 h on TiO_2,[32] and 2 days on goethite.[28,33] To clarify the sorption process of Th(IV) in PAMS12, the pseudo-first-order kinetic model, the pseudo-second-order kinetic model, and the intraparticle diffusion model were applied to analyze the experimentally observed kinetic data, respectively. The model details and parameters, as well as the correlation coefficient obtained by the three models are listed in Supporting Information SI-6. The fitting curves are denoted by different line styles in Figure 8b. From the good fitting with correlation coefficient of more than 0.999 and the fact that the sorption capacity (q_e) obtained from pseudo-second-order model (141 mg/g) is very close to the experimentally observed equilibrium capacity (140 mg/g), it can be clearly concluded that the sorption of Th(IV) in PAMS follows a pseudo-second-order

Table 3. Comparison of Parameters of Langmuir, Freundlich, and Dubinin−Radusckevich Isotherms

isotherm model									
Langmuir			Freundlich			Dubinin−Radusckevich			
Q_m(mg/g)	b (mL/mg)	R^2	k_F (mg/g)	n	R^2	Q_m (mg/g)	β (mol^2/kJ^2)	E (kJ/mol)	R^2
181	0.116	0.99	48	3.5	0.96	427	2.6×10^{-3}	13.9	0.96

model regardless of reaching equilibrium or not. Besides, it is observed that in the initial several minutes for the highest sorption kinetics, the experimental data also fit well with the intraparticle diffusion model, suggesting that intraparticle diffusion plays an important role for the rate determination in the Th(IV) sorption by PAMS12. This is understandble for a nanoparticle sorbent with porous structure.

Sorption isotherm is fundamental in understanding the sorption mode of sorbate on sorbent surface once the equilibrium attains. In the present study, the amount of Th(IV) sorbed in PAMS12 as a function of Th(IV) concentration in supernatant at the equilibrium state (C_e), i.e., sorption isotherm, was determined at a constant pH of 3.5 ± 0.1 by varying initial Th(IV)concentration ($[Th]_{initial}$) from 0 to 160 mg/L. The results are shown in Figure 8c. The Th(VI) sorption by PAMS12 is found to has a sharp increase at a C_e of <5 mg/L, corresponding to ca. 80 mg/g of sorption, after which the sorption comes to a mild increase with Th(IV) concentration greater than 5 mg/L. When $[Th]_{initial}$ is more than 120 mg/L, corresponding to a C_e of ca. 50 mg/L, the sorbent is saturated by Th(IV) and the maximum sorption capacity of 166 mg/g was established. It is noted that beyond the sorption capacity of 80 mg/g, the C_e clearly exceeds the maximum concentration limit of WHO set for Th(IV) in drinking water, from which the effective sorption capacity of PAMS12 for Th(IV) during the purification of water was deemed as less than 80 mg/g, a value of one-half of the saturated sorption capacity. To identify the sorption mode of Th(IV) in PAMS12, the isotherm data were applied to three commonly used models, Langmuir model, Freundlich model and Dubinin−Radusckevich (D-R) model. The model and fitting details are presented in Supporting Information SI-7. The fitting curves are shown by different line styles in Figure 8c and the fitting parameters are list in Table 3. It is clear from the fitting that the Th(IV) sorption in PAMS12 follows Langmuir model very well, revealing a monolayer uniform sorption mode. And a mean free energy (E) of 13.9 kJ/mol obtained from D-R fitting unambiguously indicates a chemisorption process.[34] All the fitting results are in good agreement with our expectation that Th(IV) ions are sorbed mainly through complexation with the phosphonate group on the surface of the sorbent.

Finally, we assess the feasibility of the PAMS sorbent applied to wastewater cleaning or recovery of Th(IV) from wastewater. The effect of ionic strength on the Th(IV) sorption by PAMS12 was studied in the presence of $NaClO_4$ with concentrations varying from 5×10^{-4} to 0.6 mol/L, as Na^+ is a common cation in the environment and $[ClO_4]^-$ is a weak coordinative anion for Th(IV).[15] To ease the influence of ionic strength by $Th(NO_3)_4$, especially at low concentrations of $NaClO_4$, a low $[Th]_{initial}$ of 20 mg/L was used and a corresponding $m_{sorbent}/V_{solution}$ of 0.1 mg/mL was chosen to achieve an appropriate Th(IV) uptake. The results are shown in Figure 8d. It is observed that the effect of ionic strength on the sorption is insignificant even at the $NaClO_4$ concentration more than 0.5 mol/L. The results are interesting and important. It is well-known that the salt concentration is very high in wastewater. The independent ionic strength sorption of Th(IV) on PAMS12 at high salt concentrations is critical for the application of PAMS in wastewater cleaning or recovery of Th(IV) from wastewater.

Th(IV) Desorption and Stability Assessment of the Sorbent. The desorption of Th(IV) from PAMS12 was performed using different concentrations of HNO_3 as eluent. The experiment Details are shown in Supporting Information SI-8, and the quantitative desorption of Th(IV) from PAMS12 using various concentrations of HNO_3 is listed in Table 4. As

Table 4. Desorption of Th(IV) from PAMS12 by HNO_3 Solution

$[HNO_3]$ (mol/L)	0.01	0.02	0.05	0.1	0.2
efficiency (%)	89	94	~99	~99	>99

can be seen, the desorption of Th(IV) from PAMS12 clearly enhances with the increasing of the concentration of HNO_3. When the concentration of HNO_3 reaches 0.2 M, a complete recovery (>99%) of the sorbed Th(IV) is achieved. As mentioned above, the Th(IV) sorption by PAMS12 is pH-dependent. At pH 1.1, for example, almost no sorption of Th(IV) occurs. From this point of view, the desorption of Th(IV) from PAMS12 can be explained as a cation exchange between protons and the Th(IV) ions. The result in the present study is similar with that in U(VI) sorption by phosphonate-functionalized mesoporous silica.[16]

To assess stability of the PAMS12 sorbent during Th(IV) sorption and desorption, the XRD patterns of as-synthesized PAMS12, Th(IV)-loaded PAMS12 and PAMS12 after desorption were compared. As shown in Figure 9. the XRD patterns for all the test samples shows one sharp peak in the

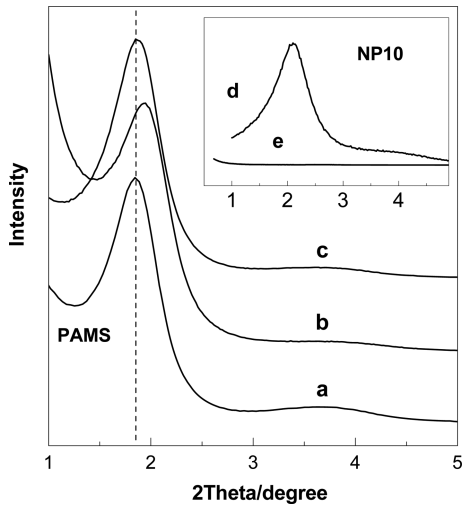

Figure 9. XRD patterns of (a) as-synthesized PAMS12, (b) Th(IV)-loaded PAMS12, and (c) PAMS12 after desorption. Inset shows XRD patterns of NP10 (d) before and (e) after U(VI) sorption.

dx.doi.org/10.1021/am405584h | ACS Appl. Mater. Interfaces 2014, 6, 4786−4796

range of 2θ close to 2.0 and one broad peak in the region of 2θ = 3−5°, which clearly reveals the maintenance of ordered mesoporous structure for both Th (IV)-loaded PAMS12 and PAMS12 after desorption and further indicates a good stability of the PAMS12 sorbent during Th(IV) sorption and desorption. In our previous work, the pores of the NP10 sorbent were blocked by the sorbed U(VI) ions during the sorption as evidenced by the loss of all XRD scattering reflections (inset of Figure 9). In this work, however, the sorbed Th(IV) ions do not block the pores of the PAMS12 sorbent, which is a guarantee that more Th(IV) ions can enter into the inner cavity of the sorbent and bind the complexation ligand there. Besides, it is noticed that for Th (IV)-loaded PAMS12, the sharp peak at 2θ close to 2.0 shifts slightly toward larger 2θ. This is understandable because the sorbed Th (IV) ions arouse a reduction of pore size of the sorbent.

Selectivity Test. To evaluate the selectivity of PAMS sorbents for Th (IV), the competitive sorption of Th(IV) by PAMS12 from the aqueous solution containing a range of competing metal ions, including Zn^{2+}, Pb^{2+}, Co^{2+}, Ni^{2+}, Sr^{2+}, Cr^{3+}, La^{3+}, Ce^{3+}, Cs^{+}, and Eu^{3+}, was performed at pH 3.5 ± 0.1, in which the concentration of all the metal ions was identical as 0.65 mmol/L. The result is shown in Figure 10. As can be seen,

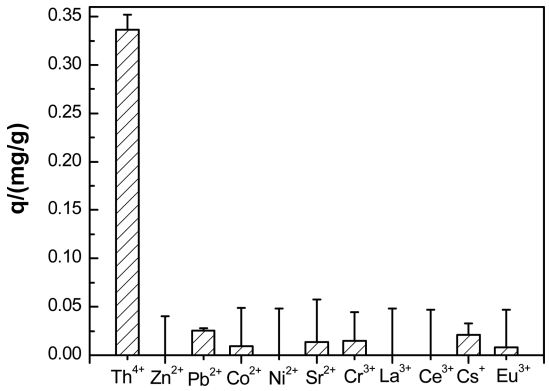

Figure 10. Competitive sorption of coexistent ions by PAMS12.

the uptake of Th(IV) in PAMS12 is more than 0.32 mmol/g, while that of other metal ions is less than 0.05 mmol/L. It is known that selectivity coefficient is commonly used to assess selectivity of sorbent for metal ions. Herein, the selectivity coefficient ($S_{Th/M}$) for Th(IV) relative to competing ions is defined as[35]

$$S_{Th/M} = \frac{K_d^{Th}}{K_d^{M}} \quad (1)$$

where K_d^{Th} and K_d^{M} are distribution ratio of Th(VI) and competing ions in sorbent and solution, respectively. It is found that the $S_{Th/M}$ value for Th(IV) relative to all the competing ions is more than 20, Which suggests that the PAMS sorbents shows a desirable selectivity for Th(IV) ions over a range of competing metal ions. The selectivity of PAMS for Th(IV) should be attributed to the complexation of phosphonate group on the sorbent. It is well-known that the oxygen of phosphonate readily binds actinides and shows desirable selectivity for Th(IV), U(VI), and Pu(IV) ions. Tri-n-butyl phosphate (TBP), for example, has been applied for several decades in extraction of U(VI) and Pu(IV) from wastewater in PUREX process. The selectivity of phosphonate for Th(IV), U(VI), and Pu(IV) ions can be rationalized from the following two aspects. One is the hsab principle. The oxygen of phosphonate is known to be a hard base, while Th(IV), U(VI) and Pu(IV) ions are hard acid. It is understandable that the hard base prefer to bind the hard acid. Another is electrostatic interaction. The oxygen of phosphonate shows strong electronegativity, which is thus more favored by highly charged cations, i.e. Th(IV), U(VI), and Pu(IV) ions.

CONCLUSIONS

In this work, we report the first study of enhanced Th(IV) sorption by using phosphonate-amino bifunctionalized mesoporous silica (PAMS). The PAMS sorbents, with ordered mesoporous structure, uniform pore diameter and large surface area, were prepared by a simple one-step co-condensation method using commonly used reagents. During Th(IV) sorption, amino group serves as "access ligand" through its hydrophilicity and thus compatibility with the hydrated metal ions, while phosphonate group is responsible for the complexation. The combination of the two groups at a relatively low coverage in PAMS arouses an enhancement of Th(IV) sorption compared to phosphonate alone functionalized and amino alone functionalized counterparts. By changing the raw material ratio in the reaction mixture, different amounts of phosphonate and amino groups were anchored to the surface of the sorbents, leading to a decrease or further enhancement of Th(IV) sorption. Besides, from the fast sorption kinetics of less than 1 h, the large sorption capacity of more than 160 mg/g at a relatively low pH, desirable selectivity for Th(IV) ions over a range of competing metal ions, and the fact that the sorbed Th(IV) can be completely desorbed by using 0.2 mol/L or more concentrated nitric acid solution, it is clearly concluded that phosphonate-amino bifunctionalized mesoporous silica, i.e., PAMS, is indeed an efficient and feasible sorbent for Th(IV) uptake from aqueous solution. This study indicates a better scope by introducing multifunctionality into mesoporous silica for the separation, removal, or recovery of actinides ions from environment. Further works are in progress to fabricate more effective actinides sorbent by combining with different functional groups into mesoporous matrix, and to assess reusability and radiation stability of these new materials for further assessing their feasibility applied in separation of actinides.

ASSOCIATED CONTENT

Supporting Information

Detailed description of analytical techniques and Th(IV) sorption experiments; thermal analyses and N_2 sorption/desorption measurement for contrast materials; Aqueous speciation of Th(IV) as a function of pH; Th(IV) sorption data fitting by kinetics models and isotherm models, and experimental procedure of Th(IV) desorption. This material is available free of charge via the Internet at http://pubs.acs.org/.

AUTHOR INFORMATION

Corresponding Authors

*E-mail: shiwq@ihep.ac.cn. Fax: 86-10-88235294. Tel: 86-10-88233968.
*E-mail: zfchai@suda.edu.cn.

Present Addresses

[†]Beijing Synchrotron Radiation Facility, Institute of High Energy Physics, Chinese Academy of Sciences, Beijing 100049, China

[‡]School of Radiological & Interdisciplinary Sciences, Soochow University, Suzhou 215123, China

Notes

The authors declare no competing financial interest.

■ ACKNOWLEDGMENTS

We are grateful to the staff of Beijing Synchrotron Radiation Facility (BSRF) and Shanghai Synchrotron Radiation Facility (SSRF) for EXAFS measurement. This work was supported by the National Natural Science Foundation of China (91326202, 11105162, 91126006, 11275219, 21201166, and 21261140335) and the "Strategic Priority Research Program" of the Chinese Academy of Sciences (Grants XDA03010401 and XDA03010403).

■ REFERENCES

(1) Jung, H.; Kwon, B. J.; Ku, J. Y.; Yu, K. H.; Ko, J. E. Preparation and Characterization of Carbamoylphosphonate(CMPO) Silane Grafted on Various Mesoporous Silicas. *J. Phys. Chem. Solids* **2010**, *71*, 663−668.

(2) Ma, Y. H.; Xing, L.; Zheng, H. Q.; Che, S. N. Anionic-Cationic Switchable Amphoteric Monodisperse Mesoporous Silica Nanoparticles. *Langmuir* **2011**, *27*, 517−520.

(3) Zhang, H. X.; Liu, X. Y.; Zhu, L.; Zhao, T.; Lan, J. F.; Yan, W. F. Synthesis and Characterization of Sulfonic Acid-Functionalized SBA-15 for Adsorption of Biomolecules. *Microporous Mesoporous Mater.* **2011**, *142*, 614−620.

(4) Su, B. L.; Yang, X. Y.; Leonard, A.; Lemaire, A.; Tian, G. Self-Formation Phenomenon to Hierarchically Structured Porous Materials: Design, Synthesis, Formation Mechanism and Applications. *Chem. Commun.* **2011**, *47*, 2763−2786.

(5) Sanchez, C.; Boissiere, C.; Grosso, D.; Chaumonnot, A.; Nicole, L. Aerosol Route to Functional Nanostructured Inorganic and Hybrid Porous Materials. *Adv. Mater.* **2011**, *23*, 599−623.

(6) Anwander, R.; Liang, Y. C.; Hanzlik, M. Periodic Mesoporous Organosilicas: Mesophase Control via Binary Surfactant Mixtures. *J. Mater. Chem.* **2006**, *16*, 1238−1253.

(7) Lee, J. F.; Thirumavalavan, M.; Wang, Y. T.; Lin, L. C. Monitoring of the Structure of Mesoporous Silica Materials Tailored Using Different Organic Templates and Their Effect on the Adsorption of Heavy Metal Ions. *J. Phys. Chem. C* **2011**, *115*, 8165−8174.

(8) Yousefi, S. R.; Ahmadi, S. J.; Shemirani, F.; Jamali, M. R.; Salavati-Niasari, M. Simultaneous Extraction and Preconcentration of Uranium and Thorium in Aqueous Samples by New Modified Mesoporous Silica prior to Inductively Coupled Plasma Optical Emission Spectrometry Determination. *Talanta* **2009**, *80*, 212−217.

(9) Walcarius, A.; Mercier, L. Mesoporous Organosilica Adsorbents: Nanoengineered Materials for Removal of Organic and Inorganic Pollutants. *J. Mater. Chem.* **2010**, *20*, 4478−4511.

(10) Lebed, P. J.; de Souza, K.; Bilodeau, F.; Lariviere, D.; Kleitz, F. Phosphonate-Functionalized Large Pore 3-D Cubic Mesoporous (KIT-6) Hybrid as Highly Efficient Actinide Extracting Agent. *Chem. Commun.* **2011**, *47*, 11525−11527.

(11) Lin, Y. H.; Fiskum, S. K.; Yantasee, W.; Wu, H.; Mattigod, S. V.; Vorpagel, E.; Fryxell, G. E.; Raymond, K. N.; Xu, J. D. Incorporation of Hydroxypyridinone Ligands into Self-assembled Monolayers on Mesoporous Supports for Selective Actinide Sequestration. *Environ. Sci. Technol.* **2005**, *39*, 1332−1337.

(12) Ghasemi, J. B.; Zolfonoun, E. Simultaneous Spectrophotometric Determination of Trace Amounts of Uranium, Thorium, and Zirconium using the Partial Least Squares Method After Their Preconcentration by Alpha-Benzoin Oxime Modified Amberlite XAD-2000 Resin. *Talanta* **2010**, *80*, 1191−1197.

(13) Lin, C. R.; Wang, H. Q.; Wang, Y. Y.; Cheng, Z. Q. Selective Solid-phase Extraction of Trace Thorium(IV) using Surface-grafted Th(IV)-imprinted Polymers with Pyrazole Derivative. *Talanta* **2010**, *81*, 30−36.

(14) Jain, V. K.; Pandya, R. A.; Pillai, S. G.; Shrivastav, P. S. Simultaneous Preconcentration of Uranium(VI) and Thorium(IV) from Aqueous Solutions using a Chelating Calix[4]arene Anchored Chloromethylated Polystyrene Solid Phase. *Talanta* **2006**, *70*, 257−266.

(15) Zuo, L. M.; Yu, S. M.; Zhou, H.; Tian, X.; Jiang, J. Th(IV) Adsorption on Mesoporous Molecular Sieves: Effects of Contact time, Solid Content, pH, Ionic Strength, Foreign Ions and Temperature. *J. Radioanal. Nucl. Chem.* **2011**, *288*, 379−387.

(16) Yuan, L. Y.; Liu, Y. L.; Shi, W. Q.; Lv, Y. L.; Lan, J. H.; Zhao, Y. L.; Chai, Z. F. High Performance of Phosphonate-Functionalized Mesoporous Silica for U(VI) Sorption from Aqueous Solution. *Dalton Trans.* **2011**, *40*, 7446−7453.

(17) Liu, Y. L.; Yuan, L. Y.; Yuan, Y. L.; Lan, J. H.; Li, Z. J.; Feng, Y. X.; Zhao, Y. L.; Chai, Z. F.; Shi, W. Q. A High Efficient Sorption of U(VI) From Aqueous Solution using Amino-Functionalized SBA-15. *J. Radioanal. Nucl. Chem.* **2012**, *292*, 803−810.

(18) Kim, J. M.; Kwak, J. H.; Jun, S.; Ryoo, R. Ion-Exchange and Thermal-Stability of Mcm-41. *J. Phys. Chem.* **1995**, *99*, 16742−16747.

(19) Ryoo, R.; Kim, J. M. Structural Order in Mcm-41 Controlled by Shifting Silicate Polymerization Equilibrium. *J. Chem. Soc., Chem. Commun.* **1995**, 711−712.

(20) Yuan, L. Y.; Liu, Y. L.; Shi, W. Q.; Li, Z. J.; Lan, J. H.; Feng, Y. X.; Zhao, Y. L.; Yuan, Y. L.; Chai, Z. F. A Novel Mesoporous Material for Uranium Extraction, Dihydroimidazole Functionalized SBA-15. *J. Mater. Chem.* **2012**, *22*, 17019−17026.

(21) Seco, F.; Hennig, C.; de Pablo, J.; Rovira, M.; Rojo, I.; Marti, V.; Gimenez, J.; Duro, L.; Grive, M.; Bruno, J. Sorption of Th(IV) onto Iron Corrosion Products: EXAFS Study. *Environ. Sci. Technol.* **2009**, *43*, 2825−2830.

(22) Dahn, R.; Scheidegger, A. M.; Manceau, A.; Curti, E.; Baeyens, B.; Bradbury, M. H.; Chateigner, D. Th Uptake on Montmorillonite: A Powder and Polarized Extended X-ray Absorption Fine Structure (EXAFS) Study. *J. Colloid Interface Sci.* **2002**, *249*, 8−21.

(23) Dacheux, N.; Clavier, N.; Wallez, G.; Quarton, M. Crystal Structures of $Th(OH)PO_4$, $U(OH)PO_4$ and $Th_2O(PO_4)_2$. Condensation Mechanism of M-IV$(OH)PO_4$ (M = Th, U) into $M_2O(PO_4)_2$. *Solid State Sci.* **2007**, *9*, 619−627.

(24) Alexandratos, S. D.; Zhu, X. P. Polyols as Scaffolds in the Development of Ion-Selective Polymer-Supported Reagents: The Effect of Auxiliary Groups on the Mechanism of Metal Ion Complexation. *Inorg. Chem.* **2008**, *47*, 2831−2836.

(25) Mohandas, J.; Kumar, T.; Rajan, S. K.; Velmurugan, S.; Narasimhan, S. V. Introduction of Bifunctionality into the Phosphinic Acid Ion-Exchange Resin for Enhancing Metal Ion Complexation. *Desalination* **2008**, *232*, 3−10.

(26) Alexandratos, S. D.; Natesan, S. Ion-Selective Polymer-Supported Reagents: the Principle of Bifunctionality. *Eur. Polym. J.* **1999**, *35*, 431−436.

(27) Teksoz, S.; Acar, C.; Unak, P. Hydrolytic Behavior of Th^{4+}, UO_2^{2+}, and Ce^{3+} Ions at Various Temperatures. *J. Chem. Eng. Data* **2009**, *54*, 1183−1188.

(28) Anirudhan, T. S.; Rijith, S.; Tharun, A. R. Adsorptive Removal of Thorium(IV) from Aqueous Solutions using Poly(methacrylic acid)-Grafted Chitosan/Bentonite Composite Matrix: Process Design and Equilibrium Studies. *Colloids Surf., A* **2010**, *368*, 13−22.

(29) Neck, V.; Kim, J. I. Solubility and Hydrolysis of Tetravalent Actinides. *Radiochim. Acta* **2001**, *89*, 1−16.

(30) Chen, C. L.; Zhao, D. L.; Feng, S. J.; Chen, S. H.; Xu, D.; Wang, X. K. Adsorption of Thorium(IV) on MX-80 Bentonite: Effect of pH, Ionic Strength and Temperature. *Appl. Clay Sci.* **2008**, *41*, 17−23.

(31) Wang, M. M.; Tao, X. Q.; Song, X. P. Effect of pH, Ionic Strength and Temperature on Sorption Characteristics of Th(IV) on

Oxidized Multiwalled Carbon Nanotubes. *J. Radioanal. Nucl. Chem.* **2011**, *288*, 859−865.
(32) Guo, Z. J.; Niu, L. J.; Tao, Z. Y. Sorption of Th(IV) Ions onto TiO_2: Effects of Contact Time, Ionic Strength, Thorium Concentration and Phosphate. *J. Radioanal. Nucl. Chem.* **2005**, *266*, 333−338.
(33) Li, Y.; Fan, Q. H.; Wu, W. S. Sorption of Th(IV) on Goethite: Effects of pH, Ionic strength, FA and Phosphate. *J. Radioanal. Nucl. Chem.* **2011**, *289*, 865−871.
(34) Saeed, M. M.; Ahmed, M.; Chaudary, M. H.; Gaffar, A. Kinetics, Thermodynamics, and Sorption Profile of Eu(III) and Tm(III) on 4-(2-pyridylazo) Resorcinol (PAR) Imbedded Polyurethane Foam. *Solvent Extr. Ion Exch.* **2003**, *21*, 881−898.
(35) Rao, T. P.; Preetha, C. R.; Gladis, J. M.; Venkateswaran, G. Removal of Toxic Uranium from Synthetic Nuclear Power Reactor Effluents using Uranyl Ion Imprinted Polymer Particles. *Environ. Sci. Technol.* **2006**, *40*, 3070−3074.